SCIENTIFIC REPORTS

OPEN

SUBJECT AREAS:
ANTENNA COMPLEX
MOLECULAR BIOPHYSICS
MOLECULAR IMAGING
PHOTOSYNTHESIS

Received
9 July 2013

Accepted
9 September 2013

Published
3 October 2013

Correspondence and requests for materials should be addressed to M.I. (miwai@riken.jp)

* Current address: Nanosystem Research Institute, National Institute of Advanced Industrial Science and Technology, 1-1-1 Higashi, Tsukuba, Ibaraki 305-8565, Japan

Photosystem II antenna phosphorylation-dependent protein diffusion determined by fluorescence correlation spectroscopy

Masakazu Iwai[1,2], Chan-Gi Pack[3], Yoshiko Takenaka[4]*, Yasushi Sako[1,3] & Akihiko Nakano[1,5]

[1]Live Cell Molecular Imaging Research Team, Extreme Photonics Research Group, RIKEN Center for Advanced Photonics, 2-1 Hirosawa, Wako, Saitama 351-0198, Japan, [2]PRESTO, Japan Science and Technology Agency, 4-1-8 Honcho, Kawaguchi, Saitama 332-0012, Japan, [3]Cellular Informatics Laboratory, RIKEN, 2-1 Hirosawa, Wako, Saitama 351-0198, Japan, [4]Flucto-Order Functions Research Team, RIKEN Advanced Science Institute, 2-1 Hirosawa, Wako, Saitama 351-0198, Japan, [5]Department of Biological Sciences, Graduate School of Science, University of Tokyo, Bunkyo-ku, Tokyo 113-0033, Japan.

Flexibility of chloroplast thylakoid membrane proteins is essential for plant fitness and survival under fluctuating light environments. Phosphorylation of light-harvesting antenna complex II (LHCII) is known to induce dynamic protein reorganization that fine-tunes the rate of energy conversion in each photosystem. However, molecular details of how LHCII phosphorylation causes light energy redistribution throughout thylakoid membranes still remain unclear. By using fluorescence correlation spectroscopy, we here determined the LHCII phosphorylation-dependent protein diffusion in thylakoid membranes isolated from the green alga *Chlamydomonas reinhardtii*. As compared to the LHCII dephosphorylation-induced condition, the diffusion coefficient of LHCII increased nearly twofold under the LHCII phosphorylation-induced condition. We also verified the results by using the LHCII phosphorylation-deficient mutant. Our observation suggests that LHCII phosphorylation-dependent protein reorganization occurs along with the changes in the rate of protein diffusion, which would have an important role in mediating light energy redistribution throughout thylakoid membranes.

Under natural fluctuations in light environments, green plants and algae fine-tune the light-harvesting system in chloroplast thylakoid membranes to maintain the optimal conditions of photosystems[1]. When light absorption in photosystem II (PSII) exceeds that in photosystem I (PSI), the intersystem electron carrier plastoquinone, turns to the reduced state. The accumulation of the reduced plastoquinone induces the phosphorylation of light-harvesting antenna complex II (LHCII)[2], which consequently leads to the decline of light absorption in PSII[3]. Without LHCII phosphorylation in the mutant lacking the Stt7 kinase, PSII excitation remains constantly higher than PSI, resulting in the energy imbalance between the two photosystems[4]. LHCII phosphorylation is thus essential for light energy redistribution between the two photosystems, or state transitions[5,6].

It has long been proposed that LHCII phosphorylation causes dynamic protein reorganization that involves both PSI and PSII[7]. Biochemical studies have revealed that LHCII phosphorylation promotes the dissociation of LHCII from PSII[8] and also the association of LHCII with PSI[9]. The capability of LHCII association with the two photosystems has been directly observed by single particle electron microscopy[10,11]. Moreover, several lines of evidence have suggested that the phosphorylation induces the migration of LHCII between two different regions of thylakoid membranes–from the stacked grana to the unstacked stroma lamellae, where PSII and PSI predominantly exist, respectively[12–15]. Despite the significance of LHCII migration in state transitions, the molecular details of how LHCII phosphorylation affects the protein diffusion in thylakoid membranes have remained unknown. Since the localization and dynamics of LHCII have important roles in the signal transduction involved with its phosphorylation[16], the investigation of LHCII diffusivity is essential to reveal the spatiotemporal information of LHCII migration in thylakoid membranes.

To determine LHCII phosphorylation-dependent protein diffusion, we here used fluorescence correlation spectroscopy (FCS). FCS has been widely used since its first measurement with a confocal microscopy setup[17].

FCS defines a tiny diffraction-limited detection volume (~0.1 fL) by a focused laser and a confocal pinhole and then detects the temporal fluctuation of fluorescence intensity as fluorescent proteins move into and out of the fixed detection volume. By fitting theoretical models to the autocorrelation of the observed fluorescence fluctuations, the diffusion coefficients can be calculated[18]. Although FCS cannot detect immobile or very slowly mobile proteins, it can determine relatively fast protein movements on a scale of microseconds (~300 $\mu m^2\ s^{-1}$)[19–21]. Since FCS has not been used to study the diffusion of chlorophyll-binding proteins (CBPs), we first confirmed the applicability of FCS by measuring the purified LHCII, the most abundant CBP in thylakoid membranes. Then, we determined the CBP diffusion in the unstacked thylakoid membrane that was purified from *Chlamydomonas reinhardtii*. We investigated the influence of LHCII phosphorylation to the CBP diffusion by manipulating the redox state of plastoquinone and also by using the LHCII phosphorylation-deficient mutant, *stt7*. Our FCS analysis provided the evidence for a variety of protein diffusion occurring in thylakoid membranes, which is regulated by LHCII phosphorylation-dependent processes.

Results

FCS measurements of purified LHCII. As the standard control for diffusion analysis in this work, a fluorescent cyanine dye, Cy5, in aqueous buffer was analyzed by FCS. The typical time-course of Cy5 fluorescence is shown (**Fig. 1a**). The diffusion coefficient of Cy5 has been extensively studied and thus known to be ~280 $\mu m^2\ s^{-1}$ (**Fig. 1c**; refs. 22, 23). Using the same experimental condition, we next measured chlorophyll (Chl) fluorescence of purified LHCII in aqueous buffer. LHCII was purified from *C. reinhardtii* by means of sucrose density gradient centrifugation. The typical time-course of Chl fluorescence fluctuations of the purified LHCII is shown (**Fig. 1b**). If observed fluorescence fluctuations were not originated from diffusion but noise, the fluorescence autocorrelation functions (FAFs) cannot be obtained[24]. In our FCS measurements, we could obtain the Chl FAFs from the observed fluorescence fluctuations that were originated from the LHCII diffusion in aqueous buffer (**Fig. 1d**). By fitting the model equation to the obtained Chl FAFs, we could determine the diffusion coefficient (D) of the LHCII in aqueous buffer–D = ~27.6 $\mu m^2\ s^{-1}$. These results demonstrated that FCS can be used to analyze protein diffusion by measuring Chl fluorescence fluctuations.

Induction of state transitions and isolation of unstacked thylakoid membranes. To simply and directly examine the lateral CBP diffusion, we isolated thylakoid membranes from *C. reinhardtii*. Also, to investigate the relationship between state transitions and changes in the CBP diffusion, we treated cells with 3-(3,4-dichlorophenyl)-1, 1-dimethylurea (DCMU) or carbonyl cyanide m-chlorophenyl hydrazone (CCCP), both of which are well-documented substances to induce the oxidized or reduced plastoquinone pool (the conditions also called state 1 or state 2), respectively[25]. After mild cell disruption, we carried out the sequential centrifugation to purify the membranes with the lowest density, typically stroma lamellae. We confirmed the membrane thickness of the isolated membranes by using atomic force microscopy (AFM), which can assess the height of samples in nanometer scale. AFM analysis indicated that the average thickness of the membranes isolated from cells in state 1 and state 2 was 14.8 ± 0.6 and 14.5 ± 1.2 nm, respectively (**Fig. S1**). These were in agreement with the thickness of the unstacked thylakoid membrane comprised of a vesicle[26]. Although the distinction between grana and stroma lamellae in *C. reinhardtii* is not as evident as that of higher plants, AFM analysis verified that the membranes to be analyzed in this work were stroma lamellae.

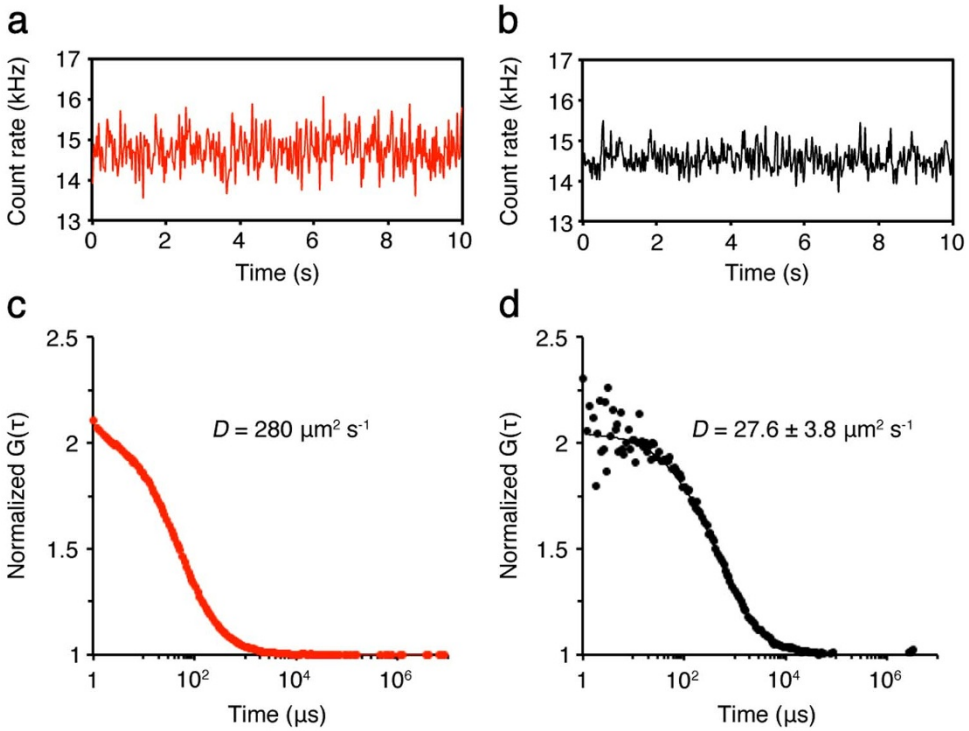

Figure 1 | FCS measurements of Cy5 and the purified LHCII in solution. Typical stationary time-courses of fluorescence fluctuations emitted from Cy5 (a) and the purified LHCII (b), both in solution, were shown. Both were measured in a coverglass chamber. (c, d) From the obtained FAFs (dots), the mean diffusion coefficients (D) of both samples were calculated by fitting the FAFs with the one-component model (lines) (see equation 2 in Methods). To obtain the diffusion coefficient of the purified LHCII, the published diffusion coefficient for Cy5 (280 $\mu m^2\ s^{-1}$) was used for the standard[22,23].

FCS measurements of the CBPs in thylakoid membranes. FCS measurement is essentially based on photon-counting experiments, in which the change in fluorescence signal from a diffraction-limited illuminated volume reflects the change in the number of fluorescent molecules within that volume[18]. Thus, FCS is not sensitive to a photobleaching or nonfluctuating signal, which is typically originated from an immobile protein or a high background. In case of the isolated thylakoid membranes, high Chl fluorescence background would hinder the precise measurements of Chl fluorescence fluctuations. Therefore, to obtain the large Chl fluorescence fluctuations, we began FCS measurements after Chl fluorescence background became low enough to evaluate the fluctuating signals (**Fig. S2**). This method is particularly effective to distinguish mobile proteins in the immobile fractions with high fluorescence intensity[27,28]. The effect of this method on protein diffusion should be minimal because only the diffraction-limited detection volume was illuminated with laser whose intensity was weak enough to prevent damage to the CBPs outside of that volume. Within the confocal detection volume, only the large and/or immobile protein complexes, such as PSII[29], were photobleached as indicated by the gradual decrease in Chl fluorescence background (**Fig. S2**). Therefore, we did not measure such immobile CBPs. What FCS actually measured was the other CBPs moving into and out of the fixed confocal detection volume (**Fig. 2a**)[27,28]. These highly mobile CBPs were not affected by the weak laser illumination because the dwell time in the confocal detection volume was extremely short. On the other hand, immobile CBPs outside of the confocal detection volume would not generate any signals in FCS analysis because they did not move into that volume. As a consequence, FCS selectively measured the protein diffusion of highly mobile CBPs in thylakoid membranes.

After decreasing the fluorescence background, we measured Chl fluorescence fluctuations in the isolated stroma lamellae. The typical time-course of Chl fluorescence fluctuations was observed, suggesting that the CBP diffusion occurred in the membrane (**Fig. 2b**). We could also obtain the Chl FAFs from the observed fluorescence fluctuations. By fitting the model equation to the obtained Chl FAFs, the

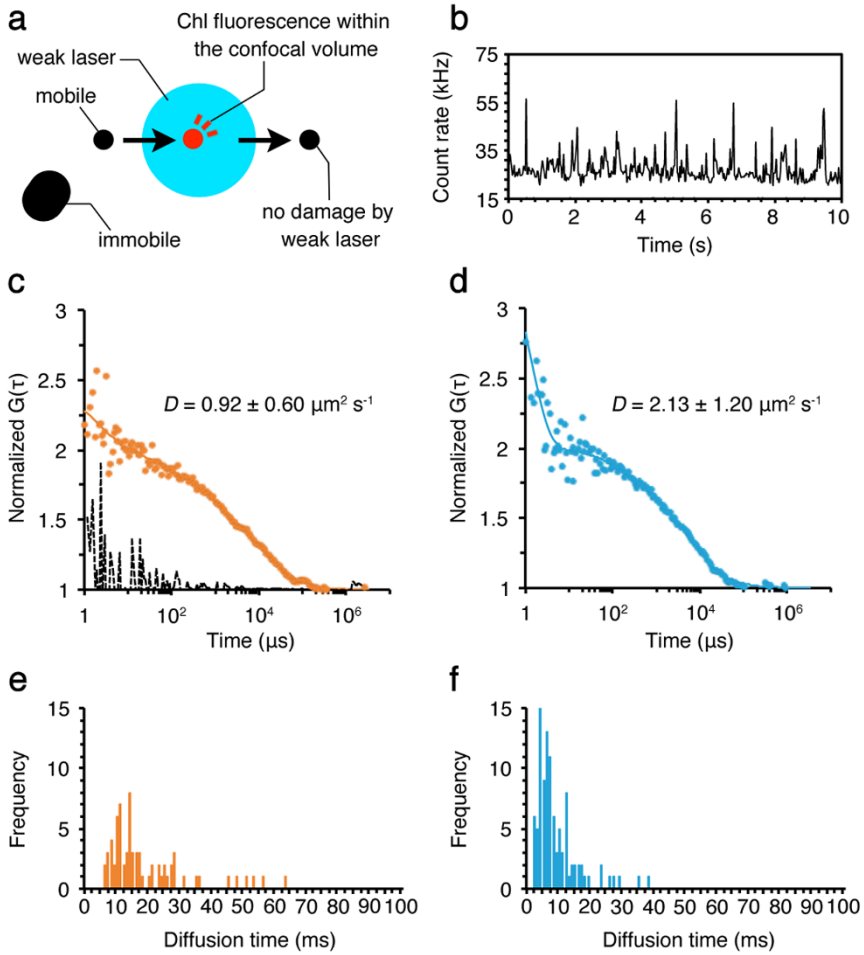

Figure 2 | FCS measurements of the CBPs in the stroma lamellae isolated from wild type. (a) The top view diagram of FCS measurements using the isolated membrane. A mobile protein (a black circle) moves into the confocal detection volume (a blue circle), where the protein (a red circle) emits fluorescence. The fluorescence signal is not detected after the protein moves out of the confocal volume. The weak laser does not cause damage to the protein moving quickly through the confocal volume. The large, immobile protein (a black oblong) in the membrane does not emit fluorescence because it does not move into the confocal volume, and thus no photobleaching occurs. (b) A typical stationary time-course of Chl fluorescence fluctuations observed by using the isolated stroma lamellae. The FAFs (dots) obtained from Chl fluorescence fluctuations were used to calculate the diffusion coefficients (D) of the CBPs in the membrane in state 1 (c) and state 2 (d) by curve fitting with a one- or two-component model with triplet term (lines) (see equation 2 in Methods). The broken line in (c) was measured as a negative control for the random signals observed outside of the analyzed membranes, which indicated no correlation, confirming that we did not measure protein diffusion leaked from membranes. The decay faster than 2 μs in FAFs is caused by the afterpulsing of detector[58], which has no effect on the diffusion coefficients we observed here. The diffusion time of the CBPs in the membrane in state 1 (e) and state 2 (f) was also measured by FCS. Distribution of mobile CBPs with certain diffusion time is shown. The calculation was done by using the 30 sets of data obtained during the total of 5 min measurements in each membrane.

mean diffusion coefficient of the CBPs in state 1 membranes showed ~0.92 $\mu m^2 s^{-1}$ (**Fig. 2c**). On the other hand, by using the membranes isolated from cells in state 2, the mean diffusion coefficient showed ~2.13 $\mu m^2 s^{-1}$, nearly twofold higher than estimated in state 1 membranes (**Fig. 2d**). FCS can directly measure the diffusion time, which represents the average transit time of mobile CBPs through the confocal detection volume. The results indicated that the membranes in state 1 contained a proportion of CBPs passing through the detection volume in about 10 ms or slower (**Fig. 2e**). In case of state 2, however, it was mostly faster than 10 ms (**Fig. 2f**). These results imply that the CBP diffusion actively occurs in the isolated stroma lamellae, and the accelerated diffusion rate in state 2 would be most likely due to LHCII phosphorylation-dependent processes. We measured the signals from outside of the membrane, in which no FAF was obtained, confirming that our FCS results did not indicate protein diffusion floating on coverglass or in buffer solution (**Fig. 2c**, a broken line).

LHCII phosphorylation-dependent CBP diffusion. Because LHCII phosphorylation is known to regulate state transitions, we examined LHCII phosphorylation levels in the isolated stroma lamellae. The purified LHCII from each isolated membrane was separated by sodium dodecyl sulfate polyacrylamide gel electrophoresis, and protein phosphorylation was detected by immunoblotting using an anti-phosphothreonine antibody (**Fig. 3a**). The results indicated that quantified phosphorylation levels of LHCII became high from state 1 to state 2 (**Fig. 3b**). The increase in phosphorylation levels of monomeric LHCII (CP26 and CP29) was also evident, especially pronounced for CP29, which is known to be essential for LHCII association with PSI in state 2[30,31] and thus considered to be redistributed during state transitions[9,16]. Therefore, the result implied that the CBP mobility in stroma lamellae was affected by the phosphorylation levels of not only trimeric LHCII but also monomeric LHCII (CP26 and CP29).

Since LHCII phosphorylation is regulated by the Stt7 kinase[4], we next investigated the CBP diffusion by using thylakoid membranes isolated from the *stt7* mutant. The stroma lamellae were purified from the *stt7* mutant similarly as described above. FCS measurements were also performed in the same experimental condition as described above. By using the stroma lamellae of the *stt7* mutant, we could obtain the FAFs, suggesting that there was certain protein diffusion occurring in this mutant as well. By fitting the model equation to the obtained Chl FAFs, we determined the mean diffusion coefficient of the CBPs in the *stt7* mutant, showing ~0.91 $\mu m^2 s^{-1}$ (**Fig. 4a**), which was comparable to the results obtained using wild type in state 1 (**Fig. 2c**). The observed diffusion time of the *stt7* mutant was mostly around 10 ms or slower (**Fig. 4b**), which was also similar to the results obtained using wild type in state 1 (**Fig. 2e**). These results confirmed that the accelerated CBP diffusion observed in stroma lamellae in state 2 did not occur without LHCII phosphorylation.

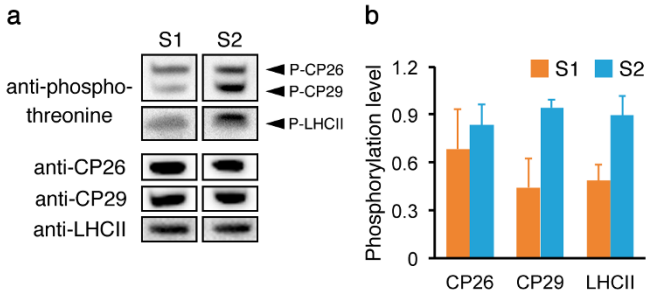

Figure 3 | Quantified LHCII phosphorylation levels in the stroma lamellae. LHCII isolated from the stroma lamellae in state 1 (S1) and state 2 (S2) was used. (a) The representative result of the immunoblotting using an anti-phosphothreonine antibody was shown. Proteins were normalized to the protein amount of LHCII. The protein amount of CP26 and CP29 was also determined by immunoblotting. Each band for S1 and S2 was derived from the same samples on the same experiment. The blots for each protein were cropped for clarity. The full length run of the blot is shown in Fig. S3. (b) The phosphorylation levels of CP26, CP29, and LHCII determined by immunoblotting were quantified using ImageJ software. Values are means of five independent experiments (±SD) and normalized to the highest value obtained in each immunoblotting.

It is well-known that the chemical treatments to induce state transitions are effective to observe the energy redistribution in *C. reinhardtii*[25], but we were not sure how these treatments affected the protein diffusion in thylakoid membranes. To confirm whether chemical treatments used in this work caused any possible artifacts to the observed CBP diffusion, we performed FCS measurements by using the *stt7* mutant treated with DCMU or CCCP. The results indicated no apparent effect on the CBP diffusion by the chemical treatments (**Fig. S4**). The diffusion coefficients observed in the membranes with chemical treatments were similar to the results obtained without the treatments. These results strongly suggested that chemical manipulation of the redox condition of plastoquinone was not efficient enough to change the protein diffusion with deficiency of Stt7, implying that LHCII phosphorylation is highly required for the acceleration of the CBP diffusion in stroma lamellae. We also confirmed that the acceleration of the CBP diffusion occurred in the membranes isolated from the wild-type cells incubated anaerobically in the dark (**Fig. S5**), which is an alternative method to induce state 2 condition in *C. reinhardtii*[32]. This also verified the acceleration of the CBP diffusion caused by another LHCII phosphorylation-induced condition. Therefore, the accelerated CBP diffusion observed in stroma lamellae in state 2 was not an artifact by the chemical treatments but LHCII phosphorylation-dependent protein diffusion.

Discussion

According to the previous studies, LHCII phosphorylation in thylakoid membranes causes its lower and higher affinity to PSII and PSI, respectively[33–35], inducing LHCII migration from grana to stroma lamellae[13]. By using FCS, we showed that LHCII phosphorylation causes acceleration of the CBP diffusion in stroma lamellae. The observed CBP diffusion reflects most likely LHCII diffusion for the following reasons: i) LHCII is the most abundant CBP in thylakoid membranes[36]; ii) we analyzed the CBP diffusion in the purified stroma lamellae, where PSII is less abundant than PSI[37]; iii) the observation of PSI fluorescence by FCS is limited due to the very short fluorescence lifetime at room temperature[38], so the effect of PSI on diffusion analysis would be minimal; and iv) even if the two photosystems are present, the slow or immobile protein diffusion of such large protein complexes is excluded from our FCS analysis (**Fig. S2**). Although the drawback of FCS is its incapability to detect slow protein diffusion, we utilized it as an effective filter to selectively evaluate highly mobile proteins, such as LHCII in thylakoid membranes.

We should mention, however, that the diffusion coefficients of LHCII determined by our FCS analysis are about two-order of magnitude higher than the ones previously observed by using single particle tracking[39]. This could imply that there are at least two different diffusion rates for the LHCII mobility—the fast one can be observed by FCS, but the other was too slow diffusion to be measured by FCS. It is also possible that such differences are due to the labeling of LHCII with a 0.8-μm diameter bead used by single particle tracking technique, which is roughly 100 times larger than a trimeric LHCII[40]. In our case, we simply observed Chl fluorescence fluctuation, so our estimation of the diffusion coefficients by using FCS should reflect the innate condition for protein diffusion. We would also like to mention that diffusion analysis by measuring the rate of fluorescence recovery after photobleaching is different from our FCS analysis in terms of spatiotemporal resolution. It has been known that FCS is better suited to fast protein movements on a scale

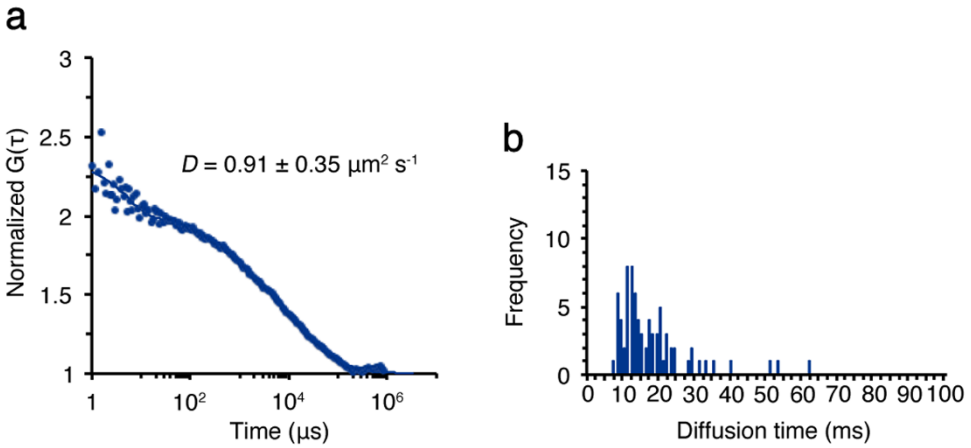

Figure 4 | FCS measurements of the CBPs in the stroma lamellae isolated from the *stt7* mutant. FCS measurements were similarly done as in Fig. 2. (a) The FAFs (dots) obtained from Chl fluorescence fluctuations were used to calculate the diffusion coefficients (*D*) of the CBPs in the membrane isolated from the *stt7* mutant. (b) The diffusion time of the CBPs in the membrane of the *stt7* mutant was measured by FCS.

of microseconds[19–21,41]. Thus, it is common that the protein diffusion observed by FCS cannot be observed by fluorescence recovery after photobleaching technique, especially in case of measuring high Chl fluorescence, which generates too much difference in fluorescence intensity after photobleaching to detect low signals originated from small and highly mobile proteins[42,43].

It is well-defined by the Stokes–Einstein equation (equation 4 in Methods) that smaller molecules move faster than larger ones. If so, one of the possible reasons for the acceleration of the CBP diffusion observed in state 2 would be the dispersal of monomeric LHCII from grana to stroma lamellae. As suggested previously, LHCII phosphorylation causes the dissociation of LHCII, migrating from grana to stroma lamellae[7]. The dissociating LHCII includes not only trimeric LHCII but also monomeric LHCII (CP26 and CP29)[8]. We observed the phosphorylation levels of monomeric LHCII increased in state 2 stroma lamellae (**Fig. 3**), which is consistent with previous studies[9]. Therefore, accelerated CBP diffusion observed in state 2 could reflect the increase in the number of monomeric LHCII in the stroma lamellae. This observation is reasonable because monomeric LHCII functions as the linker between trimeric LHCII and PSI[9,30], so the number of monomeric LHCII has to be increased in stroma lamellae, where the formation of PSI-LHCI-LHCII supercomplex occurs in state 2[10,11]. This supercomplex formation is another possible reason for the accelerated CBP diffusion as it decreases the excluded volume and generates more available spaces for mobile proteins[44–46]. Because dynamic protein-protein interactions regulate processes for the optimization of photosynthesis[47], the spatial availability in the membrane is the important factor to efficiently regulate the supercomplex formation. Therefore, the accelerated CBP diffusion observed by our FCS measurements could indicate the increase in the spatial availability in stroma lamellae. These observations suggest that the membrane condition of stroma lamellae is extremely fluid, where the rate of protein diffusion is readily modulated by LHCII phosphorylation. Such mobile conditions of stroma lamellae might be advantageous for molecular interactions efficiently taken place to regulate photoacclimation mechanisms.

Since thylakoid membranes inside cells are far more complex and heterogeneous in terms of the length, thickness, protein composition and organization, it would be challenging to discern the changes in protein mobility *in vivo*. In this work, we demonstrate the LHCII phosphorylation-dependent CBP diffusion at the single-molecule level by the combination of the membrane purification and the measurement of protein diffusion in the membranes. Although it is currently impossible to measure the protein mobility of each one of the different membrane proteins simultaneously, we could show the existence of highly mobile CBPs in stroma lamellae, which were under control of LHCII phosphorylation. Flexibility of thylakoid membrane protein organization has shown to be important for not only state transitions but also the switch between linear and cyclic electron flows[48], excess light energy dissipation mechanism[49], and PSII repair mechanism[50]. Therefore, further investigations of the protein mobility in thylakoid membranes would deepen our understanding for the flexible machinery of chloroplast light-harvesting system.

Methods

Strains and growth condition. *C. reinhardtii* wild type strain 137c and the *stt7* mutant (a kind gift from J.-D. Rochaix, University of Geneva) were grown in Tris-acetate-phosphate liquid media[51] under low light (~20 μmol photons m^{-2} s^{-1}) at 23°C. Induction of state transitions was done as described previously[8,25,32].

Isolation of stroma lamellae. The procedure to isolate thylakoid membranes was essentially the same as described previously[8], except for the following. After mild cell disruption in MS buffer (25 mM MES, pH 6.5/NaOH, 0.33 M sucrose, and 1.5 mM NaCl) by using BioNeb system (Glas-Col) at 10 kgf/cm^2 on ice, thylakoid membranes were subjected to sucrose cushion centrifugation (0.33/1.3/1.8 M sucrose with 25 mM MES, pH 6.5/NaOH, 1.5 mM NaCl) at 131,500 × *g* for 30 min at 4°C. The membranes concentrated in the upper phase (between 0.33 M and 1.3 M sucrose) were collected. After dilution with MS buffer, the collected membranes were centrifuged at 27,000 × *g* for 10 min at 4°C once. The supernatant was collected and centrifuged again at 27,000 × *g* for 30 min at 4°C. The obtained pellet was resuspended and used in this work. For AFM and FCS, the obtained membranes were diluted with filtered MES buffer (25 mM MES, pH 6.5/NaOH) and centrifuged at 27,000 × *g* for 10 min at 4°C once. The Chl amount was measured by Porra method[52], and the Chl concentration of the membranes was adjusted to 0.25 μg Chl/μL by using filtered MES buffer. The membranes were used immediately for AFM and FCS sample preparation without freeze-thaw.

LHCII purification and phosphorylation analysis. Purification of LHCII was done as described previously[9]. Immunoblotting was performed as described previously[53]. Antibodies were kindly given by Dr. J. Minagawa at National Institute of Basic Biology (anti-CP26 and anti-CP29)[9] and Dr. M. Hippler at University of Münster [anti-LHCII (LhcbM6)[54]]. A commercially available antibody was used for anti-phosphothreonine (Cell Signaling).

AFM. A mica disc attached to a slide glass using a two-component araldite glue (Devcon Epoxy; ITW) was used as a support. The freshly cleaved mica surface was immediately covered by 40 μL of adsorption buffer (10 mM Tris, pH 7.3/HCl, 150 mM KCl, 20 mM $MgCl_2$) as described previously[55]. Then, 20 μL of freshly prepared thylakoid membrane solution (0.25 μg Chl/μL) was added to the adsorption buffer on the mica surface and incubated for 10 min. The mica surface was gently rinse with 1 mL of MilliQ water and blown by nitrogen stream to remove excess water. AFM images were acquired by using a commercial MFP-3D Stand Alone AFM in tapping mode in air (Asylum Research). Silicon cantilevers with a length of 240 μm (k = 2 N/m; OMCL-AC240TS-C2, Olympus) were used. AFM data were analyzed by using the Asylum Research AFM IGOR Pro software (Wavemetrics). Averaged height was calculated from the membrane areas of at least 50 μm^2.

FCS. The bottom surface of an 8-well chambered coverglass (Nunc) was covered by 40 μL of adsorption buffer as described above. Then, 20 μL of freshly prepared thylakoid membranes (0.25 μg Chl/μL) were added to the adsorption buffer on the coverglass surface and incubated for 10 min. The surface was gently rinsed with 500 μL of MilliQ water once and then covered with 40 μL of recording buffer (10 mM Tris, pH 7.3/HCl, 150 mM KCl). The membranes attached to the coverglass surface were observed by using a LSM510 ConfoCor2 confocal laser scanning microscope (Carl Zeiss). We used the membranes with the equal size for each measurement. Chl pigments in the isolated membranes were excited at 633 nm with a CW He-Ne laser (~2 μW) through a water immersion objective lens (C-Apochromat, 40 × 1.2 NA, Carl Zeiss), and the emission was detected through a 650-nm longpass filter.

FCS measurements of the CBPs in the membranes and the data analysis were done as described previously[56]. Briefly, Chl FAFs [G(τ)] were calculated as:

$$G(\tau) = 1 + \frac{\langle \delta I(t) \bullet \delta I(t+\tau) \rangle}{\langle I(t) \rangle^2}, \quad (1)$$

where τ, $I(t)$, and G(τ) indicate time delay and fluorescence intensity, respectively. The acquired G(τ) values were fitted using a one-, two-, or three-component model:

$$G(\tau) = 1 + \frac{1}{N} \sum_i F_i \left(1 + \frac{\tau}{\tau_i}\right)^{-1} \left(1 + \frac{\tau}{s^2 \tau_i}\right)^{-1/2}, \quad (2)$$

where F_i and τ_i are the fraction and diffusion time of component i, respectively; N is the average number of Chl fluorescent molecules existed in the excited confocal detection volume defined by the radius w_0 and the length $2z_0$; and s is the structure parameter representing the ratio $s = z_0/w_0$. The s was calibrated using the published diffusion coefficient (280 $\mu m^2\ s^{-1}$) of Cy5 in solution at room temperature[22,23]. The confocal pinhole diameter was adjusted to 70 μm to minimize the confocal detection volume. The excitation laser power was adjusted so that high enough signal-to-noise ratio was obtained for diffusion analysis, and the photobleaching of Chl pigments was also minimized. Chl fluorescence fluctuations were measured for 10 s sequentially. We measured at least 5 different membranes, and the data were collected from the total of ~5 min measurement (*i.e.* the 30 data sets were obtained for each sample). For all experiments, the control measurement at the blank region near the analyzed membrane was also done to confirm no leak of CBPs from membranes into the buffer solution (**Fig. 2c**). All measured Chl FAFs were fit with the software installed on the ConfoCor2 system using the model described above. To estimate diffusion coefficients, FAFs of CBPs in the membranes were fit to a one- or two- component model (i = 1 or 2) with additional triplet or blinking terms. Chl FAFs of the solubilized LHCII in solution were well fit to a one-component model (i = 1). For two-dimensional fitting, the structure parameter was set to 1000 or much higher values[41,57]. Chl FAFs obtained from the membrane contained the signal for fast blinking, which corresponds to apparent diffusion coefficients higher than 30 $\mu m^2\ s^{-1}$ (faster than that of purified LHCII in buffer solution). Thus, the apparent fast blinking signal was excluded from the statistical analysis. Data containing photobleaching resulting from immobile membrane proteins were excluded from the diffusion analysis as described previously[27,28] (see also **Fig. S2**). The diffusion time, τ, for the component i is related to the translational diffusion coefficient D of the component i by

$$\tau_i = \frac{w_{xy}^2}{4D_i}. \quad (3)$$

The diffusion coefficient of a molecule is related to various physical parameters according to the Stokes–Einstein equation, as follows:

$$D_i = \frac{\kappa_B T}{6\pi\eta r_i}, \quad (4)$$

where κ_B is Boltzmann constant, T is absolute temperature, η is fluid-phase viscosity of the solvent, and r_i is the hydrodynamic radius of molecules. The diffusion coefficients of CBPs in the membranes and in solution were calculated from the published diffusion coefficient for Cy5 (280 $\mu m^2\ s^{-1}$)[22,23] and samples, as the following equation:

$$\frac{D_{sample}}{D_{Cy5}} = \frac{\tau_{Cy5}}{\tau_{sample}}. \quad (5)$$

1. Niyogi, K. K. & Truong, T. B. Evolution of flexible non-photochemical quenching mechanisms that regulate light harvesting in oxygenic photosynthesis. *Curr. Opin. Plant Biol.* **16**, 1–8 (2013).
2. Zito, F. *et al.* The Qo site of cytochrome b6f complexes controls the activation of the LHCII kinase. *EMBO J.* **18**, 2961–2969 (1999).
3. Allen, J. F., Bennet, J., Steinback, K. E. & Arntzen, C. J. Chloroplast protein phosphorylation couples plastoquinone redox state to distribution of excitation energy between photosystems. *Nature* **291**, 21–25 (1981).
4. Depege, N., Bellafiore, S. & Rochaix, J. D. Role of chloroplast protein kinase Stt7 in LHCII phosphorylation and state transition in *Chlamydomonas*. *Science* **299**, 1572–1575 (2003).
5. Wollman, F. A. State transitions reveal the dynamics and flexibility of the photosynthetic apparatus. *EMBO J.* **20**, 3623–3630 (2001).
6. Minagawa, J. State transitions–the molecular remodeling of photosynthetic supercomplexes that controls energy flow in the chloroplast. *Biochim. Biophys. Acta* **1807**, 897–905 (2011).
7. Allen, J. F. State transitions–a question of balance. *Science* **299**, 1530–1532 (2003).
8. Iwai, M., Takahashi, Y. & Minagawa, J. Molecular remodeling of photosystem II during state transitions in *Chlamydomonas reinhardtii*. *Plant Cell* **20**, 2177–2189 (2008).
9. Takahashi, H., Iwai, M., Takahashi, Y. & Minagawa, J. Identification of the mobile light-harvesting complex II polypeptides for state transitions in *Chlamydomonas reinhardtii*. *Proc. Natl. Acad. Sci. USA* **103**, 477–482 (2006).
10. Kouřil, R. *et al.* Structural characterization of a complex of photosystem I and light-harvesting complex II of *Arabidopsis thaliana*. *Biochemistry* **44**, 10935–10940 (2005).
11. Kargul, J. *et al.* Light-harvesting complex II protein CP29 binds to photosystem I of *Chlamydomonas reinhardtii* under State 2 conditions. *FEBS J.* **272**, 4797–4806 (2005).
12. Andersson, B., Akerlund, H. E., Jergil, B. & Larsson, C. Differential phosphorylation of the light-harvesting chlorophyll protein complex in appressed and non-appressed regions of the thylakoid membrane. *FEBS Lett.* **149**, 181–185 (1982).
13. Kyle, D. J., Staehelin, L. A. & Arntzen, C. J. Lateral mobility of the light-harvesting complex in chloroplast membranes controls excitation energy distribution in higher plants. *Arch. Biochem. Biophys.* **222**, 527–541 (1983).
14. Bassi, R., Giacometti, G. M. & Simpson, D. J. Changes in the organization of stroma membranes induced by in vivo state 1 state 2 transition. *Biochim. Biophys. Acta* **935**, 152–165 (1988).
15. Delosme, R., Olive, J. & Wollman, F. A. Changes in light energy distribution upon state transitions: An in vivo photoacoustic study of the wild type and photosynthesis mutants from *Chlamydomonas reinhardtii*. *Biochim. Biophys. Acta* **1273**, 150–158 (1996).
16. Rochaix, J. D. Role of thylakoid protein kinases in photosynthetic acclimation. *FEBS Lett.* **581**, 2768–2775 (2007).
17. Rigler, R., Mets, U., Widengren, J. & Kask, P. Fluorescence correlation spectroscopy with high count rate and low-background - analysis of translational diffusion. *Eur. Biophys. J.* **22**, 169–175 (1993).
18. Haustein, E. & Schwille, P. Single-molecule spectroscopic methods. *Curr. Opin. Struct. Biol.* **14**, 531–540 (2004).
19. Politz, J. C., Browne, E. S., Wolf, D. E. & Pederson, T. Intranuclear diffusion and hybridization state of oligonucleotides measured by fluorescence correlation spectroscopy in living cells. *Proc. Natl. Acad. Sci. USA* **95**, 6043–6048 (1998).
20. Wachsmuth, M. *et al.* Analyzing intracellular binding and diffusion with continuous fluorescence photobleaching. *Biophys. J.* **84**, 3353–3363 (2003).
21. Milan-Lobo, L. *et al.* Subtype-specific differences in corticotropin-releasing factor receptor complexes detected by fluorescence spectroscopy. *Mol. Pharmacol.* **76**, 1196–1210 (2009).
22. Bark, N., Foldes-Papp, Z. & Rigler, R. The incipient stage in thrombin-induced fibrin polymerization detected by FCS at the single molecule level. *Biochem. Biophys. Res. Commun.* **260**, 35–41 (1999).
23. Mozziconacci, J., Sandblad, L., Wachsmuth, M., Brunner, D. & Karsenti, E. Tubulin dimers oligomerize before their incorporation into microtubules. *PLoS One* **3**, e3821 (2008).
24. Madge, D., Elson, E. & Webb, W. W. Thermodynamic fluctuations in a reacting systemMeasurement by fluorescence correlation spectroscopy. *Phys. Rev. Lett.* **29**, 705–708 (1972).
25. Bulte, L., Gans, P., Rebeille, F. & Wollman, F. A. ATP control on state transitions in vivo in *Chlamydomonas reinhardtii*. *Biochim. Biophys. Acta* **1020**, 72–80 (1990).
26. Daum, B. & Kuhlbrandt, W. Electron tomography of plant thylakoid membranes. *J. Exp. Bot.* **62**, 2393–2402 (2011).
27. Bacia, K., Majoul, I. V. & Schwille, P. Probing the endocytic pathway in live cells using dual-color fluorescence cross-correlation analysis. *Biophys. J.* **83**, 1184–1193 (2002).
28. Weidemann, T. *et al.* Counting nucleosomes in living cells with a combination of fluorescence correlation spectroscopy and confocal imaging. *J. Mol. Biol.* **334**, 229–240 (2003).
29. Kirchhoff, H., Haferkamp, S., Allen, J. F., Epstein, D. B. & Mullineaux, C. W. Protein diffusion and macromolecular crowding in thylakoid membranes. *Plant Physiol.* **146**, 1571–1578 (2008).
30. Tokutsu, R., Iwai, M. & Minagawa, J. CP29, a monomeric light-harvesting complex II protein, is essential for state transitions in *Chlamydomonas reinhardtii*. *J. Biol. Chem.* **284**, 7777–7782 (2009).
31. Turkina, M. V. *et al.* Environmentally modulated phosphoproteome of photosynthetic membranes in the green alga *Chlamydomonas reinhardtii*. *Mol. Cell Proteomics* **5**, 1412–1425 (2006).
32. Finazzi, G., Barbagallo, R. P., Bergo, E., Barbato, R. & Forti, G. Photoinhibition of *Chlamydomonas reinhardtii* in State 1 and State 2: damages to the photosynthetic apparatus under linear and cyclic electron flow. *J. Biol. Chem.* **276**, 22251–22257 (2001).
33. Croce, R., Breton, J. & Bassi, R. Conformational changes induced by phosphorylation in the CP29 subunit of photosystem II. *Biochemistry* **35**, 11142–11148 (1996).

34. Nilsson, A. *et al.* Phosphorylation controls the three-dimensional structure of plant light harvesting complex II. *J. Biol. Chem.* **272**, 18350–18357 (1997).
35. Zer, H. *et al.* Regulation of thylakoid protein phosphorylation at the substrate level: reversible light-induced conformational changes expose the phosphorylation site of the light-harvesting complex II. *Proc. Natl. Acad. Sci. USA* **96**, 8277–8282 (1999).
36. Peter, G. F. & Thornber, J. P. Biochemical composition and organization of higher plant photosystem II light-harvesting pigment-proteins. *J. Biol. Chem.* **266**, 16745–16754 (1991).
37. Akerlund, H. E. & Andersson, B. Quantitative separation of spinach thylakoids into photosystem-II-enriched inside-out vesicles and photosystem-I-enriched right-side-out vesicles. *Biochim. Biophys. Acta* **725**, 34–40 (1983).
38. Wendler, J. & Holzwarth, A. R. State transitions in the green alga *Scenedesmus Obliquus* probed by time-resolved chlorophyll fluorescence spectroscopy and global data analysis. *Biophys. J.* **52**, 717–728 (1987).
39. Consoli, E., Croce, R., Dunlap, D. D. & Finzi, L. Diffusion of light-harvesting complex II in the thylakoid membranes. *EMBO Rep.* **6**, 782–786 (2005).
40. Jansson, S. The light-harvesting chlorophyll a/b-binding proteins. *Biochim. Biophys. Acta* **1184**, 1–19 (1994).
41. Adkins, E. M. *et al.* Membrane mobility and microdomain association of the dopamine transporter studied with fluorescence correlation spectroscopy and fluorescence recovery after photobleaching. *Biochemistry* **46**, 10484–10497 (2007).
42. Feder, T. J., Brust-Mascher, I., Slattery, J. P., Baird, B. & Webb, W. W. Constrained diffusion or immobile fraction on cell surfaces: a new interpretation. *Biophys. J.* **70**, 2767–2773 (1996).
43. Verkman, A. S. Solute and macromolecule diffusion in cellular aqueous compartments. *Trends Biochem. Sci.* **27**, 27–33 (2002).
44. Ellis, R. J. Macromolecular crowding: obvious but underappreciated. *Trends Biochem. Sci.* **26**, 597–604 (2001).
45. Marenduzzo, D., Finan, K. & Cook, P. R. The depletion attraction: an underappreciated force driving cellular organization. *J. Cell Biol.* **175**, 681–686 (2006).
46. Kirchhoff, H. Molecular crowding and order in photosynthetic membranes. *Trends Plant Sci.* **13**, 201–207 (2008).
47. Eberhard, S., Finazzi, G. & Wollman, F. A. The dynamics of photosynthesis. *Annu. Rev. Genetics* **42**, 463–515 (2008).
48. Iwai, M. *et al.* Isolation of the elusive supercomplex that drives cyclic electron flow in photosynthesis. *Nature* **464**, 1210–1213 (2010).
49. Johnson, M. P. *et al.* Photoprotective energy dissipation involves the reorganization of photosystem II light-harvesting complexes in the grana membranes of spinach chloroplasts. *Plant Cell* **23**, 1468–1479 (2011).
50. Aro, E. M. *et al.* Dynamics of photosystem II: a proteomic approach to thylakoid protein complexes. *J. Exp. Bot.* **56**, 347–356 (2005).
51. Gorman, D. S. & Levine, R. P. Cytochrome *f* and plastocyanin: Their sequence in the photosynthetic electron transport chain of *Chlamydomonas reinhardtii*. *Proc. Natl. Acad. Sci. USA* **54**, 1665–1669 (1965).
52. Porra, R. J., Thompson, W. A. & Kriedemann, P. E. Determination of accurate extinction coefficients and simultaneous-equations for assaying chlorophyll-a and chlorophyll-b extracted with 4 different solvents - verification of the concentration of chlorophyll standards by atomic-absorption spectroscopy. *Biochim. Biophys. Acta* **975**, 384–394 (1989).
53. Iwai, M., Yokono, M., Inada, N. & Minagawa, J. Live-cell imaging of photosystem II antenna dissociation during state transitions. *Proc. Natl. Acad. Sci. USA* **107**, 2337–2342 (2010).
54. Stauber, E. J. *et al.* Proteomics of *Chlamydomonas reinhardtii* light-harvesting proteins. *Eukaryot. Cell* **2**, 978–994 (2003).
55. Scheuring, S. *et al.* Watching the photosynthetic apparatus in native membranes. *Proc. Natl. Acad. Sci. USA* **101**, 11293–11297 (2004).
56. Pack, C., Saito, K., Tamura, M. & Kinjo, M. Microenvironment and effect of energy depletion in the nucleus analyzed by mobility of multiple oligomeric EGFPs. *Biophys. J.* **91**, 3921–3936 (2006).
57. Ohsugi, Y., Saito, K., Tamura, M. & Kinjo, M. Lateral mobility of membrane-binding proteins in living cells measured by total internal reflection fluorescence correlation spectroscopy. *Biophys. J.* **91**, 3456–3464 (2006).
58. Zhao, M. *et al.* Afterpulsing and its correction in fluorescence correlation spectroscopy experiments. *Appl. Optics* **42**, 4031–4036 (2003).

Acknowledgements

This work was supported by JSPS KAKENHI Grant Numbers 21870047 and 23687008, JST PRESTO, and grants from RIKEN Center for Advanced Photonics, Extreme Photonics Research Project.

Author contributions

M.I., C.P. and Y.T. performed research and analyzed data. Y.S. and A.N. contributed the analytic and computational tools. M.I. designed the research and wrote the paper. All authors reviewed the manuscript.

Additional information

Supplementary information accompanies this paper at http://www.nature.com/scientificreports

Competing financial interests: The authors declare no competing financial interests.

How to cite this article: Iwai, M., Pack, C., Takenaka, Y., Sako, Y. & Nakano, A. Photosystem II antenna phosphorylation-dependent protein diffusion determined by fluorescence correlation spectroscopy. *Sci. Rep.* **3**, 2833; DOI:10.1038/srep02833 (2013).